Preprints of the 21st IFAC World Congress (Virtual)
Berlin, Germany, July 12-17, 2020

A cooperative fault-tolerant control method for the coupled system based on interaction effect utilization

Jing Chang * **Jérôme Cieslak** ** **Zongyi Guo** *** **David Henry** **

* *Xidian University, Xi'an, China (e-mail: jchang@xidian.edu.cn).*
** *University of Bordeaux, Talence 33400, France (e-mail: jerome.cieslak@ims-bordeaux.fr; david.henry@u-bordeaux.fr)*
*** *Northwestern Polytechnical University, Xi'an, China (e-mail: guozongyi@nwpu.edu.cn)*

Abstract: An active fault-tolerant control scheme is proposed in this paper for the strongly coupled MIMO systems which subject to total actuator failures. A control-oriented interaction indicator is defined in the Lyapunov stability sense and then is utilized to design the cooperative fault-tolerant control law. The proposed scheme can achieve robust tracking performance with globally uniformly ultimate boundlessness and is capable of improving transient performance (fault-tolerant ability) by wisely using the interactions. Simulation results obtained on a flight attitude control system illustrates the benefit of the proposed techniques.

Keywords: Fault tolerant control, cooperative control, interaction effect utilization.

1. INTRODUCTION

With the rapid development of unmanned autonomous systems, the past several decades have witnessed an explosive growth of Fault Detection and Diagnosis (FDD), Fault Detection and Isolation (FDI), Fault-Tolerant Control (FTC) and Fault-Tolerant Guidance (FTG) in most disciplines of engineering to enhance the safety of the system in case of the occurrence of unknown fault/failure, see Zolghadri et al. (2014). And particularly, safety is a critical issue in the area of aircraft and aerospace industry, where the FDI, fault-tolerant flight control have been widely developed (Gao and Wang (2014)). Reliable control systems are needed more than ever in the face of rising autonomous and intelligent levels, increasing advancement and complexity of aircraft and aerospace vehicles, the opportunities and challenges presented by new technologies (distributed, networked and cooperative). Despite the high number of published works about fault-tolerant control, too few works take into account the total actuator failures.

Control Allocation (CA) is an efficient approach for dealing with total actuator failures without the reconfiguration of the controller (Alwi and Edwards (2008)). However, it is hard to consider the uncertain control effectiveness and obtain the optimized CA.On the other hand, the CA method required the invertible of the control distribution matrix, which is not always held for the serious actuator faults. As for a faulty system within total actuator failures, it sometimes becomes an underactuated system. The existence of state interactions and control interactions in the MIMO system is a form of coupling. The strong coupling exists in some MIMO systems (see Weiland et al. (2004); Tian et al. (2013)) which results in difficulty to control the system in fast maneuvering motions, such as rapid descent and fast lateral maneuver of flight. For the normal case, the decoupling control scheme (Dhadekar and Patre (2017)) and decentralized control scheme (Dickeson et al. (2009)) can help in easily and directly designing the controller, since it allows the designer to set the controller for each state independent of the other states. When applicable, the advantage of completely decentralized control is that one can apply the simpler SISO theory (Dhadekar and Patre (2017)). While this traditional design scheme essentially regards the coupling as a detrimental element in the system and eliminates or suppresses its effect on the system directly (Guo et al. (2017, 2018a)). In fact, the existence of interactions between the states or inputs of MIMO systems could be helpful to stabilize the actual motion in under-actuated systems. As for couplings acting on the MIMO systems, the fault-tolerant property of interactive effect has not been sufficiently investigated yet, nor the relationship with the expected system trajectory. In recent work (Guo et al. (2017, 2018b); Chang et al. (2018)), a novel coupling effect indicator is proposed to demonstrate the coupling effects on the system. This proposed control scheme achieved a better dynamic performance by explicitly utilizing the system couplings in the controller design. The improvements in the dynamic performance of this strategy thanks to the switching behavior triggered by the coupling effect. This control strategy is similar to the phase-based gain-modulation control that improves damping while the error is increasing and reducing the control gain while transiting toward the desired output. This motivates the work of this paper, wherein the controller is modulated according to interaction indicators to attain a certain cooperative fault-tolerant method for MIMO systems. More specifically, this paper will revisit

⋆ This work was supported by the National Natural Science Foundation of China under Grant 61803308. Corresponding author Jing Chang (jchang@xidian.edu.cn).

the state and input coupling effect and consider whether the interactions can be utilized in the fault-tolerant control design more wisely.

In this context, a cooperative FTC scheme is presented for the coupled MIMO system subjected to actuator failures. Firstly, the effect of the couplings on system stability and performance is analyzed to help with building a control-oriented interaction indicator. Then, the cooperative fault-tolerant controller based on these indicators is proposed, which can enforce and maintain the system tracking performance in the presence of actuator failures. The idea behind this scheme is to utilize the interactions to derive a control law with virtual control in Lyapunov stability sense for the coupled system. The resulting solution ensures the dynamic performance of MIMO systems in the presence of actuator failures. Simulation results obtained on the nonlinear lateral model of the flight attitude system illustrate the benefits of the proposed scheme.

The rest of the paper is organized as follows. Section II lays down problem formulation and the main results are listed in Section III. Simulation studies are illustrated in Section IV. The paper concludes in Section V.

2. PROBLEM STATEMENT

Considering the following class of nonlinear, multi-variable and strongly coupled systems, which are suitable to represent many mechatronic systems

$$\ddot{q} = f(q,\dot{q}) + g(q,\dot{q})\dot{q} + B(q)u \tag{1}$$

where $q, \dot{q} \in \mathbb{R}^n$ denotes position and velocity, $u \in \mathbb{R}^m$ denotes control input; $f(q,\dot{q}) : \mathbb{R}^n \times \mathbb{R}^n \mapsto \mathbb{R}^n$, $g(q,\dot{q}) : \mathbb{R}^n \times \mathbb{R}^n \mapsto \mathbb{R}^{n\times n}$ and $B(q) : \mathbb{R}^n \mapsto \mathbb{R}^{n\times m}$ represent the system dynamics terms. Let u_k^f represent the signal from the k-th actuator that has failed. Then the actuator fault can be described as follows:

$$u^f_{k,\sigma(t)}(t) = \lambda^f_{k,\sigma(t)}u(t) + d^f_{k,\sigma(t)}(q,\dot{q}) \tag{2}$$

where $0 \le \lambda^f_{k,\sigma(t)} \le 1$, $k = 1,2,\ldots,m$, $d^f_{k,\sigma(t)}(q,\dot{q})$ denotes a bounded signal, $\sigma(t)$ is a switching function representing the healthy and faulty controller cases. Here, when $0 \le \lambda^f_{k,\sigma(t)} \le 1$, it represents the loss of effectiveness of the actuators and $\lambda^f_{k,\sigma(t)} = 0$ if the ith actuator fails completely. The $d^f_{k,\sigma(t)}(q,\dot{q})$ is the actuator bias fault. For the sake of simplicity, in this study λ^f_k and d^f_k are used to replace $\lambda^f_{k,\sigma(t)}$, and $d^f_{k,\sigma(t)}(q,\dot{q})$, respectively. Define $\Lambda^f_\sigma = diag[\lambda^f_1, \lambda^f_2, \ldots, \lambda^f_m]$ and $d^f_\sigma(q,\dot{q}) = [d^f_1, d^f_2, \ldots, d^f_m]^T$. Let $x_1 = q, x_2 = \dot{q}$, the dynamics of system (1) can be further written as

$$\begin{cases} \dot{x}_1 = x_2 \\ \dot{x}_2 = f(x_1,x_2) + g(x_1,x_2)x_2 + B(x_1)u \end{cases} \tag{3}$$

Assumption 1. The $f(q,\dot{q})$, $g(q,\dot{q})$ and $d(q,\dot{q})$ are assumed to satisfy the local Lipschitz and the linear growth conditions, where $f(0,0) = 0$, $d(0,0) = 0$.

Assumption 2. The matrix $B(q)$ is invertible and the system (1) with fault-free is fully-actuated in configuration $(q,\dot{q},t)$, which means $rank[B(q)] = n$.

First of all, since the system (1) is in strict-feedback form, we could use backstepping technique to design the normal controller. Introduce a new variable $s = Kx_1 + x_2$, where $K = diag\{k_1, k_2, \ldots, k_n\}$ is a positive definite matrix. Using Eq.(1), the time derivative of (3) yields

$$\dot{s} = f(x_1,x_2) + Kx_2 + g(x_1,x_2)x_2 + B(x_1)u \tag{4}$$

The nominal controller with fault-free can be easily designed as:

$$u = B(x_1)^{-1}[-f(x_1,x_2) - g(x_1,x_2)x_2 - Kx_2 - Ks] \tag{5}$$

Then we have

$$\begin{bmatrix} \dot{x}_1 \\ \dot{s} \end{bmatrix} = \begin{bmatrix} -K & I \\ 0 & -K \end{bmatrix} \begin{bmatrix} x_1 \\ s \end{bmatrix} \tag{6}$$

Therefore, the system (3) is asymptotically stable in the healthy condition. If the actuator fault occurs, the dynamics of s become

$$\begin{aligned} \dot{s} = {} & f(x_1,x_2) + Kx_2 + g(x_1,x_2)x_2 + B(x_1)d^f_\sigma(x_1,x_2) + \\ & B(x_1)\Lambda^f_\sigma B(x_1)^{-1}[-f(x_1,x_2) - (K + g(x_1,x_2))x_2 - Ks] \end{aligned} \tag{7}$$

In general, after the fault occurs, the fault-tolerant control is activated as soon as actuator faults are detected and isolated. On the basis of the desired control $u(t)$ and the estimation of Λ^f_σ and d^f_σ, the fault-tolerant control u_{sk} is constructed as

$$u_{sk} = \frac{u_k - \hat{d}^f_k}{\hat{\lambda}^f_k} \tag{8}$$

where $\hat{\lambda}^f_k$, $\hat{d}^f_k$ are the estimates of λ^f_k, d^f_k respectively.

The above conventional FTC design is restrictive in the following two aspects (Shen et al. (2017)):

1) The denominator of the fault-tolerant control input (8) contains the estimation of the gain fault. If the denominator is equal to zero, such as $\hat{\lambda}^f_k = 0$, a controller singularity occurs. To avoid such singularity, the FTC scheme can be modified as $u_{sk} = \frac{\hat{\lambda}^f_k(u_k - \hat{d}^f_k)}{(\hat{\lambda}^f_k)^2 + \epsilon}$, where ϵ ($\epsilon << 1$) is a small positive constant (Shen et al. (2017)). Then the system (1) is asymptotically stable for the case $\lambda^f_k > 0$ and the state x_1, x_2 converging asymptotically to a small neighborhood. It can be observed from (8) that when $\hat{\lambda}^f_k$ is very small but much bigger than ϵ, the scale factor $\frac{\hat{\lambda}^f_k}{(\hat{\lambda}^f_k)^2 + \epsilon}$ is very large, which easily leads to the actuator saturation of real-world mechatronic systems.

2) In most fault estimation-based FTC design schemes, it assumes that $\lambda^f_k \neq 0$ or $B(x_1)\Lambda^f$ is invertible. However, as $n = m$, the stuck and float of actuator result in $\lambda^f_{k,\sigma(t_f)} = 0$, $t > t_f$, thus the irreversible of $B(x_1)\hat{\Lambda}^f$. The circuit system failure of the controller unit often causes loose connection faults, which will result in the intermittent deviation of controller output with $\lambda^f_{k,\sigma(t^f_k)} = 0, if\ t \in [t^f_k, t^{f'}_k]$. Here, t^f_k is the k-th switching instants due to the failure and the system switches to the healthy case at $t^{f'}_k$. Application of adaptive FTC in nonlinear system for the case $\lambda^f_k = 0$ and $rank[B(x_1)\Lambda^f] < n$ is still a challenge, to the best of the author's knowledge.

In view of the pertaining issues of the above FTC design, the control objective is re-defined as follows. To simply illustrate the design problem, we consider the following two-input-two-output system in this paper:

$$\begin{cases} \dot{x}_{11} = x_{21} \\ \dot{x}_{12} = x_{22} \\ \dot{x}_{21} = \underbrace{f_1(x_{11}, x_{21})}_{independent\ dynamic} + \underbrace{b_{11}(x_1)u_1}_{independent\ control} \\ \quad + \underbrace{g_1(x_1, x_2)x_{22}}_{coupled\ dynamic} + \underbrace{b_{12}(x_1)u_2}_{coupled\ control} \\ \dot{x}_{22} = \underbrace{f_2(x_{12}, x_{22})}_{independent\ dynamic} + \underbrace{b_{22}(x_1)u_2}_{independent\ control} \\ \quad + \underbrace{g_2(x_1, x_2)x_{21}}_{coupled\ dynamic} + \underbrace{b_{21}(x_1)u_1}_{coupled\ control} \end{cases} \tag{9}$$

In order to make sure the system is controllable, we assume that only one actuator totally failed at any given moment for system (9).

This work investigates the problem of fault-tolerant control for system (9), with the objective to provide a solution for stabilizing system in serious actuator faulty situations (stuck, float of the actuator). More specifically, for a given fault $u_f(t)$ and an allowed ultimate tracking accuracy $|x_1(t)| \leq \varepsilon$, the purpose of this paper is to find a cooperative fault-tolerant control $u(t)$ such that the closed-loop system is stable to face $\lambda_k^f = 0$. An interesting question arises that is how to use these interactions to stabilize the serious faulty system.

Remark 1. In general, the control distribution matrix $B(x_1)$ to be diagonally dominant matrix, where $|b_{11}(x_1)| > |b_{12}(x_1)|$ and $|b_{22}(x_1)| > |b_{21}(x_1)|$.

3. MAIN RESULTS

The basic idea of the proposed method in this paper is to use coupling effects between different subsystems to compensate for the total loss of effectiveness of specific actuators. The coupling effect is utilized as auxiliary input for the subsystem under fault to achieve the desired goal.

Before introducing the fault-tolerant controller, the effect of the interactions between the states or inputs of MIMO systems is studied in the fault recoverability analysis. First of all, to analyze how couplings influence the system in the Lyapunov stability sense, we design the baseline control as

$$\begin{aligned} u_{1o} &= \frac{1}{b_{11}(x_1)}(-k_{1s}s_1 - f_1(x_{11}, x_{21}) - k_1 x_{21}) \\ u_{2o} &= \frac{1}{b_{22}(x_1)}(-k_{2s}s_2 - f_2(x_{12}, x_{22}) - k_2 x_{22}) \end{aligned} \tag{10}$$

where $s_1 = k_1 x_{11} + x_{21}, s_2 = k_2 x_{12} + x_{22}$. Substitution of (10) into (9) yields

$$\begin{aligned} \begin{bmatrix} \dot{x}_{11} \\ \dot{s}_1 \end{bmatrix} &= \begin{bmatrix} -k_1 & 1 \\ 0 & -k_{1s} \end{bmatrix} \begin{bmatrix} x_{11} \\ s_1 \end{bmatrix} + \begin{bmatrix} 0 \\ g_1(x_1, x_2)x_{22} + b_{12}(x_1)u_2 \end{bmatrix} \\ &= A_1 z_1 + G_1(x, u_2) \\ \begin{bmatrix} \dot{x}_{12} \\ \dot{s}_2 \end{bmatrix} &= \begin{bmatrix} -k_2 & 1 \\ 0 & -k_{2s} \end{bmatrix} \begin{bmatrix} x_{12} \\ s_2 \end{bmatrix} + \begin{bmatrix} 0 \\ g_2(x_1, x_2)x_{21} + b_{21}(x_1)u_1 \end{bmatrix} \\ &= A_2 z_2 + G_2(x, u_1) \end{aligned} \tag{11}$$

where $z_1 = [x_{11}, s_1]^T, z_2 = [x_{12}, s_2]^T, x = [x_1, x_2]^T$. The A_1, A_2 are Hurwitz matrix. For the Lyapunov candidate $V_1 = \frac{1}{2} z_1^T z_1$, its derivative is given by

$$\begin{aligned} \dot{V}_1 &= \underbrace{-k_1 x_{11}^2 + x_{11}s_1 - k_{1s}s_1^2}_{\text{independent part}} + \underbrace{s_1 g_1 x_{22} + s_1 b_{12} u_2}_{\text{Interaction effect}} \\ &\leq -(k_1 - \frac{1}{4})x_{11}^2 - (k_{1s} - 1)s_1^2 + s_1 g_1 x_{22} + s_1 b_{12} u_2 \end{aligned} \tag{12}$$

Take the derivative of $V_2 = \frac{1}{2} z_2^T z_2$, we have

$$\begin{aligned} \dot{V}_2 &= \underbrace{-k_2 x_{12}^2 + x_{12}s_2 - k_{2s}s_2^2}_{\text{independent part}} + \underbrace{s_2 g_2 x_{21} + s_2 b_{21} u_1}_{\text{Interaction effect}} \\ &\leq -(k_2 - \frac{1}{4})x_{12}^2 - (k_{2s} - 1)s_2^2 + s_2 g_2 x_{21} + s_2 b_{21} u_1 \end{aligned} \tag{13}$$

Definition 1. Consider the system (9), the control-oriented state and control input coupling interaction indicators (COII) are defined as:

$$\begin{aligned} J_{s1} &= s_1 g_1 x_{22}, J_{u1} = s_1 b_{12} u_2 \\ J_{s2} &= s_2 g_2 x_{21}, J_{u2} = s_2 b_{21} u_1 \end{aligned} \tag{14}$$

It can be seen that the state couplings and control input couplings on system will determine the sign of the $\dot{V}_{1,2}$. If $J_{xi}, J_{ui} < 0$, couplings help the state toward zero. If $J_{xi}, J_{ui} > 0$, it will prevent the state convergence.

In this paper, borrowing the idea from coupling utilization and adaptive backstepping control technique developed in (Guo et al. (2018a)), we will use the cooperative control based on interaction utilization to deal with the serious actuator faults. For the two-input-two-output system (9), we only can tolerant one actuator total failure. Suppose that the actuator fault happened in u_1. When $\lambda_{1,\sigma(t_f)}^f = 0$, the state x_{11} is uncontrollable under (10). From (11), the state x_{22} can be regarded as a virtual control source for state x_{21}. Thus, the cooperative fault-tolerant control strategy is firstly designing the virtual control x_{22}^c to maintain x_{11} to a small bound, then using u_2 to control the state x_{12}. In order to make x_{12} also converge to a small value, the virtual control x_{22}^c should be zero after the state $|x_{11}| < \varepsilon$.

In terms of cooperative fault-tolerant control, the COII can be reformulated as

$$\begin{aligned} J_{x_1} &= s_1 g_1 \tilde{s}_2, J_{u_1} = s_1 b_{12} u_2, \\ J_{\tilde{s}_2} &= \tilde{s}_2 g_2 x_{21}, J_{u2} = \tilde{s}_2 b_{21} u_1 \end{aligned} \tag{15}$$

where $\tilde{s}_2 = x_{22} - x_{22}^c$. Despite the fact that estimate value $\hat{\lambda}_k^f, \hat{d}_k^f$ will not be a perfect estimate of the real one λ_k^f, d_k^f. Here, we consider an exogenous estimate for $\hat{\lambda}_k^f$ and an biased estimate of $\hat{d}_k^f$, where $\lambda_k^f = (1 - \Delta_k)\hat{\lambda}_k^f$, $\hat{d}_k^f = d_k^f + \tilde{d}_k^f$ with $|\Delta_k| < \bar{\delta}_e, |\tilde{d}_k^f| < \bar{\delta}_d$. Then, using the C_n-class functions in (Chen et al. (2015)), we will design virtual control variable and the actual control law in the following forms:

$$\begin{aligned} x_{22}^c &= \tfrac{1}{g_1}[-\eta_1 D_{\varepsilon,\epsilon,2}(s_1) - M_{\varepsilon,\epsilon,2}(s_1)(k_{1s}s_1 + \\ &\quad S_f(J_{x_1})g_1\tilde{s}_2 + S_f(J_{u1})b_{12}u_2 + f_1 + b_{11}\hat{u}_1^f \\ &\quad + k_1 x_{21})] + (1 - M_{\varepsilon,\epsilon,2}(s_1))x_{22}^d \\ x_{22}^d &= -k_2 x_{12} \end{aligned} \tag{16}$$

$$\begin{aligned} u_1 = \tfrac{1}{b_{11}\hat{\lambda}_1^f}[&-f_1 - k_1 x_{21} - k_{s1}s_1 - \eta_1 sign(s_1) \\ &- S_J(J_{s_1})g_1 x_{22} - S_J(J_{u1})b_{12}u_2] - \tfrac{\hat{d}_1^f}{\hat{\lambda}_1^f}, \hat{\lambda}_1^f \neq 0 \end{aligned} \tag{17}$$

$$u_2 = \frac{1}{b_{22}}\left[-f_2 - k_{s2}\tilde{s}_2 - \eta_2 sign(\tilde{s}_2) + \dot{x}_{22}^c - S_J(J_{\tilde{s}_2})g_2x_1 - S_J(J_{u2})b_{21}\hat{u}_1^f\right] \tag{18}$$

where the function $S_f(z)$ and $S_J(z)$ follow

$$S_f(z) = \begin{cases} S_{\varepsilon,2}(z), & z \geq 0 \\ 0, & z < 0 \end{cases}$$
$$S_J(z) = \frac{sign(z)+1}{2} = \begin{cases} 1, & z \geq 0 \\ 0, & z < 0 \end{cases} \tag{19}$$

and $\varepsilon, \epsilon, k_1, k_2$ are the design parameters, $\hat{u}_1^f = \hat{\lambda}_1^f\hat{u}_1 + \hat{d}_1^f$. It can be verified that x_{2c} is continuous and $\dot{x}_{2c}$ can be obtained by any differentiator. We used the sliding mode control term in u_1 and u_2 to achieve fast convergence. Then, the dynamics of the closed-loop system is expressed as

$$\begin{cases} \dot{x}_{11} = -k_1x_{11} + s_1 \\ \dot{s}_1 = -k_{s1}s_1 - \eta_1 sign(s_1) + G_1(s_1, \tilde{d}_1^f, \Delta_1), \lambda_1^f \neq 0 \\ \dot{s}_1 = -M_{\varepsilon,\epsilon,2}(s_1)k_{s1}s_1 - \eta_1 D_{\varepsilon,\epsilon,2}(s_1) + G_1^f(s_1, \tilde{s}_2, \tilde{u}_1^f), \lambda_1^f = 0 \\ \dot{x}_{12} = -k_2x_{12} + \tilde{s}_2 + \tilde{x}_{22} \\ \dot{\tilde{s}}_2 = -k_{s2}\tilde{s}_2 - \eta_2 sign(\tilde{s}_2) + G_2(s_1, \tilde{s}_2, \tilde{u}_1^f) \end{cases} \tag{20}$$

where

$$\begin{aligned} G_1(s_1, \tilde{d}_1^f, \Delta_1) &= (1 - S_J(J_{s_1}))g_1x_{22} + (1 - S_J(J_{u1}))b_{12}u_2 \\ &\quad \Delta_1(1-b_{11})\hat{d}_1^f - \Delta_1 b_{11}\hat{\lambda}_1^f u_1 - b_{11}\tilde{d}_1^f \\ G_1^f(s_1, \tilde{s}_2, \tilde{u}_1^f) &= (1 - M_{\varepsilon,\epsilon,2}(s_1))[f_1 + k_1x_{21} + b_{11}\hat{u}_1^f \\ &\quad - k_2x_{12}] + [1 - M_{\varepsilon,\epsilon,2}(s_1)S_f(J_{x_1})]g_1\tilde{s}_2 \\ &\quad + [1 - M_{\varepsilon,\epsilon,2}(s_1)S_f(J_{u1})]b_{12}u_2 + b_{11}\tilde{u}_1^f \\ G_2(s_1, \tilde{s}_2, \tilde{u}_1^f) &= [1 - S_J(J_{\tilde{s}_2})]g_2x_{21} + [1 - S_J(J_{u2})]b_{21}\hat{u}_1^f \\ &\quad + b_{21}\tilde{u}_1^f \\ \tilde{x}_{22} &= x_{22}^c - x_{22}^d,\ \tilde{u}_1^f = u_1^f - \hat{u}_1^f \end{aligned}$$

Remark 2. Based on the definition of $M_{\varepsilon,\epsilon,2}(x), D_{\varepsilon,\epsilon,2}(x)$, $S_f(z)$ and $S_J(z)$, it follows that:

$$zD_\varepsilon(z) = \begin{cases} |z|, & if\ |z| \geq \varepsilon \\ z\cos^2(\frac{\pi}{2}\sin^2(\frac{\pi}{2}\frac{z^2-\varepsilon^2}{\epsilon_2^2-\varepsilon^2})), & if\ \varepsilon > |z| > \epsilon \\ 0, & if\ |z| \leq \epsilon \end{cases} \tag{21}$$

$$zM_\varepsilon(z) = \begin{cases} z, & if\ |z| \geq \varepsilon \\ z\cos^n(\frac{\pi}{2}\sin^n(\frac{\pi}{2}\frac{z^2-\varepsilon_1^2}{\varepsilon_2^2-\varepsilon_1^2})), & if\ \varepsilon > |z| > \epsilon \\ 0, & if\ |z| \leq \epsilon \end{cases} \tag{22}$$

$$zS_f(z) = \begin{cases} z & if\ z > \varepsilon \\ zSgn_{\varepsilon,2}(z), & if\ \varepsilon > z \geq 0 \\ 0, & if\ z < 0 \end{cases} \tag{23}$$

$$zS_J(z) = \begin{cases} z\ \ if\ z \geq 0 \\ 0,\ if\ z < 0 \end{cases} \tag{24}$$

where $D_\varepsilon(x), M_\varepsilon(x)$ are the short hand of $D_{\varepsilon,\epsilon,2}(x)$ and $M_{\varepsilon,\epsilon,2}(x)$.

Theorem 1. Consider the system (9) subjected to actuator failure $u_1^f(t)$ modeled as (2), if the control law is designed as (17)-(18) with the virtual control variable (16), and the control gains satisfy the following relationship

$$\begin{aligned} &\eta_1 > max\{\bar{\delta}_1^e, |b_{11}|\bar{\delta}_2^e\},\ if|s_1| > \varepsilon; \\ &\eta_1 > \frac{(1-\iota_1)\bar{\delta}_1 - \bar{\delta}_2}{\iota_2},\ if|s_1| < \varepsilon \\ &\eta_2 > |b_{21}|\bar{\delta}_2^e \end{aligned} \tag{25}$$

where $\bar{\delta}_i^e, \iota_i, \bar{\delta}_i, i = 1, 2$ will be defined in the following. Then, for any bounded initial conditions, we have the following statements:

- all the signals of the closed-loop system (9) remain bounded all the time.
- the error variable $\tilde{s}_2$ converges to zero in finite time, the state s_1 satisfies $|s_1| \leq \varepsilon$ in finite time, and the state x_{11}, x_{12} are converging to a small bound.

Proof. Note that there are two kind of faults considered here, thus, the proof will be provided for two cases.

a *Loss of effectiveness fault,* $\lambda_1^f \neq 0$.

If only part of the control effectiveness lost in the u_1, we consider the Lyapunov function candidate $V_1 = \frac{1}{2}s_1^2 + \frac{1}{2}\tilde{s}_2^2$, whose derivative is easily computed as follows

$$\begin{aligned} \dot{V}_1 &= -k_{s1}s_1^2 - \eta_1|s_1| + s_1[1 - S_J(J_{\tilde{s}_1})]g_1x_{22} \\ &\quad + s_1[1 - S_J(J_{u1})]b_{12}u_2 + s_2(\Delta_1(1-b_{11})\hat{d}_1^f \\ &\quad - \Delta_1 b_{11}\hat{\lambda}_1^f u_1 - b_{11}\tilde{d}_1^f) \\ &\quad - k_{s2}\tilde{s}_2^2 - \eta_2|\tilde{s}_2| + s_2[1 - S_J(J_{\tilde{s}_2})]g_2x_{21} \\ &\quad + s_2[1 - S_J(J_{u2})]b_{21}\hat{u}_1^f + s_2b_{21}\tilde{u}_1^f \end{aligned} \tag{26}$$

Suppose the bounded fault estimation error is small, and $|\Delta_1(1-b_{11})\hat{d}_1^f - \Delta_1 b_{11}\hat{\lambda}_1^f u_1 - b_{11}\tilde{d}_1^f| < \bar{\delta}_1^e$ and $|\tilde{u}_1^f| < \bar{\delta}_2^e$. Then, with Remark 2, we have

$$\begin{aligned} \dot{V}_1 &\leq -k_{s1}s_1^2 - (\eta_1 - \bar{\delta}_1^e)|s_1| - k_{s2}\tilde{s}_2^2 \\ &\quad - (\eta_2 - |b_{21}|\bar{\delta}_2^e)|\tilde{s}_2| \\ &\leq -\nu_1V_1 - \nu_2V_1^{\frac{1}{2}} \end{aligned} \tag{27}$$

where $\eta_1 \geq \bar{\delta}_1^e, \eta_2 > |b_{21}|\bar{\delta}_2^e$ and $\nu_1, \nu_2 > 0$. Thus, the tracking errors $s_1, \tilde{s}_2$ will converge to zero in finite time, seeChang et al. (2017). After s_1 converge to zero, it is observed from (16) that $x_{22}^c = x_{22}^d$. Then, we have

$$\dot{x}_{11} = -k_1x_{11}, \quad \dot{x}_{12} = -k_2x_{12} \tag{28}$$

Therefore, the states x_{11}, x_{12} will asymptotically converge to zero in fault-free case.

b *Serious actuator fault,* $\lambda_1^f = 0$.

Then, the analysis is divided into three phases.

Phase 1: $|s_1| > \varepsilon$

Consider the Lyapunov function candidates $V_s = \frac{1}{2}s_1^2 + \frac{1}{2}\tilde{s}_2^2$, whose derivative is easily computed as follows

$$\begin{aligned} &\dot{V}_s = -\eta_1 s_1 D_\varepsilon(s_1) - k_{s1}s_1^2M_\varepsilon(s_1) + s_1(1 - M_\varepsilon(s_1)) \\ &[f_1 + k_1x_{21} + b_{11}\hat{u}_1^f - k_2x_{12}] + s_1[1 - M_\varepsilon(s_1)S_f(J_{x_1})] \\ &g_1\tilde{s}_2 + s_1[1 - M_\varepsilon(s_1)S_f(J_{u1})]b_{12}u_2 + s_1b_{11}\tilde{u}_1^f \\ &- k_{s2}\tilde{s}_2^2 - \eta_2|\tilde{s}_2| + s_2[1 - S_J(J_{\tilde{s}_2})]g_2x_{21} \\ &+ s_2[1 - S_J(J_{u2})]b_{21}\hat{u}_1^f + s_2b_{21}\tilde{u}_1^f \end{aligned} \tag{29}$$

Based on (21), then Eqs.(29) can be updated as

$$\begin{aligned} \dot{V}_s &\leq -k_{s1}s_1^2 - (\eta_1 - |b_{11}|\bar{\delta}_2^e)|s_1| \\ &\quad - k_{s2}\tilde{s}_2^2 - (\eta_2 - |b_{21}|\bar{\delta}_2^e)|\tilde{s}_2| \end{aligned} \tag{30}$$

It can be confirmed that the $\tilde{s}_2$ will converge to zero in finite time, and the variable s_1 will converge to ε in finite time, if the following relationship is satisfied

$$\eta_1 > max\{\bar{\delta}_1^e, |b_{11}|\bar{\delta}_2^e\}, \quad \eta_2 > |b_{21}|\bar{\delta}_2^e \tag{31}$$

Furthermore, x_{22}^c is bounded in finite time due to its definition. The boundness of x_{22}^c and $\tilde{s}_2$ further implies that $x_{22} = x_{22}^c + \tilde{x}_2$ is bounded. Choose the Lyapunov function candidates for x_{11}, x_{12} as $V_{x11} = \frac{1}{2}x_{11}^2, V_{x12} = \frac{1}{2}x_{12}^2$. From (20), we have $\dot{V}_{x11} \leq -(k_1|x_{11}| - s_1)|x_{11}|$ and $\dot{V}_{x12} \leq -(k_2|x_{12}| - \tilde{s}_2 - \tilde{x}_{22})|x_{12}|$. It is obvious that $\dot{V}_{x11} < 0$ if $|x|_{11} \geq \frac{|s_1|}{k_1}$, and $\dot{V}_{x12} < 0$ if $|x|_{12} \geq \frac{|\tilde{s}_2 - \tilde{x}_{22}|}{k_2}$. Thus, for this case x_{11} will converge to $\frac{\varepsilon}{k_1}$ and x_{12} will be bounded. Therefore, we conclude that all states are bounded.

Phase 2: $\epsilon < |s_1| < \varepsilon$

When $\epsilon < |s_1| < \varepsilon$, it follows that $M_\varepsilon(s_1) = \iota_1$ and $D_\varepsilon(s_1) = \iota_2 sign(s_1)$ where $0 < \iota_i < 1, i = 1, 2$. Since $\tilde{s}_2$ will converge to zero in finite time. Consider the Lyapunov candidate $V_\epsilon = V_{x11} + V_{x12} + \frac{1}{2}s_1^2$, it follows that

$$\begin{aligned}\dot{V}_\epsilon &= -k_1 x_{11}^2 + x_{11}s_1 - \eta_1\iota_2|s_1| - k_{s1}\iota_1 s_1^2 + s_1(1-\iota_1)\\ &\quad [f_1 + k_1(s_1 - k_1 x_{11}) + b_{11}\hat{u}_1^f - k_2 x_{12}] + s_1 b_{11}\tilde{u}_1^f\\ &\quad + s_1[1 - \iota_1 S_f(J_{u1})]b_{12}u_2 - k_2 x_{12}^2 - x_{12}\tilde{x}_{22}\\ &\quad \leq -(k_1|x_{11}| - \varepsilon(1 - k_1^2 + \iota_1 k_1^2))|x_{11}|\\ &\quad - (\eta_1\iota_2 - (1-\iota_1)\bar{\delta}_1 - \bar{\delta}_2)|s_1| - (k_2|x_{12}| - |\tilde{x}_{22}|)|x_{12}|\end{aligned} \tag{32}$$

where $\bar{\delta}_1 > |f_1 + b_{11}\hat{u}_1^f - k_2 x_{12}|$ and $\bar{\delta}_2 > |b_{11}\tilde{u}_1^f + (1 - \iota_1 S_f(J_{u1}))b_{12}u_2|$ when $\epsilon < |s_1| < \varepsilon$. If the relationships $|x_{11}| > \frac{\varepsilon(1+\iota_1 k_1^2 - k_1^2)}{k_1}$, $\eta_1 > \frac{(1-\iota_1)\bar{\delta}_1 - \bar{\delta}_2}{\iota_2}$ and $|x_{12}| \geq \frac{|\tilde{x}_{22}|}{k_2}$ are satisfied, $V_\epsilon < 0$ holds. Recall that the virtual control command x_{22}^c tends to x_{22}^d as $|s_1|$ decreases in this phase. Thus, $\tilde{x}_{22}$ decreases as well, which results in the decreased bound of x_{12}. Design positive constants k_1, k_2 can guarantee the convergence of s_1 to the bound ϵ.

Phase 3: $|s_1| \leq \epsilon$

If $|s_1| \leq \epsilon$, it follows that $x_{22}^c = x_{22}^d$. Thus, as $\tilde{s}_2$ converges to zero, $x_{22} = -k_2 x_{12}$. The dynamic of x_{11}, x_{12} becomes

$$\dot{x}_{11} = -k_1 x_{11} + s_1, \quad \dot{x}_{12} = -k_2 x_{12} \tag{33}$$

Then we have the $x_{12} \mapsto \frac{\epsilon}{k_1}$ and $x_{12} \to 0$ as $t \mapsto \infty$.

4. SIMULATIONS

In this section, in order to demonstrate the efficiency of the proposed method in this paper, we apply the cooperative FTC method into the flight attitude control system (Ra et al. (2013); Chwa and Choi (2001)). The simplified Lateral model of the angular velocity dynamics for the flight is given by

$$\begin{aligned}\dot{\omega}_x &= -b_1\omega_x - b_2\omega_y - b_3\beta + b_4\delta_x + b_5\delta_y\\ \dot{\omega}_y &= -c_1\omega_y - c_2\omega_x - c_3\beta + c_4\delta_x + c_5\delta_y\end{aligned} \tag{34}$$

where ω_x, ω_y represent the roll and yaw rates, β is yaw angle, and δ_x and δ_y are the aileron and rudder deflection angles. Aerodynamic coeffcients $b_i, c_i, i = 1, \ldots, 5$ are functions of $V, \alpha, \beta, \omega_y, \omega_x$, where V is the velocity, α is the angle of attack. The relative perturbations in the aerodynamics parameters are 15% of their respective nominal values, respectively. The amplitude and rate of the actuator are restricted as $-30^\circ \leq \delta_x, \delta_y \leq 30^\circ$ and $-200^\circ/s \leq \dot{\delta}_x, \dot{\delta}_y \leq 200^\circ/s$. The failure of aileron defection δ_x at $t = 1\ s$ with $\bar{\delta}_x = 1^\circ$ is considered in the simulation.

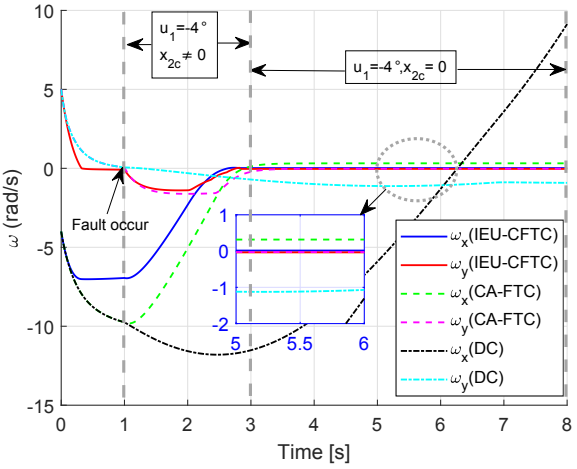

Fig. 1. Response curves of the angular velocity.

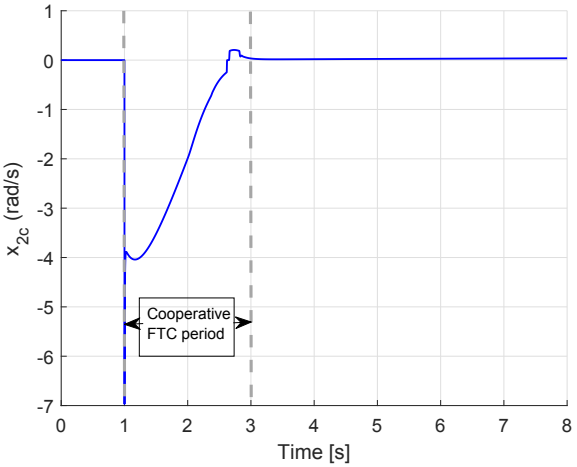

Fig. 2. Trajectories of the virtual control x_{2c}

Based on the control method proposed in Section III, the nonlinear controller is designed as

$$\begin{aligned}u_1(t) =& \frac{1}{b_4}\left[b_1\omega_x + b_2\omega_y - k_1\omega_x - b_5\delta_y\right]\\ \omega_{yc}(t) =& \frac{1}{-b_2}\left[-\eta_1 D_{\varepsilon,\epsilon,2}(\omega_x) + M_{\varepsilon,\epsilon,2}(\omega_x)\right.\\ & (-S_f(J_{\omega_x})b_2\tilde{\omega}_y - S_f(J_{u1})b_5 u_2\\ & \left. + b_1\omega_x - b_4 u_1 - k_1\omega_x)\right] w_f(t)\\ u_2(t) =& \frac{1}{c_5}\left[c_1\omega_y - k_2\tilde{\omega}_y - \eta_2 sign(\tilde{\omega}_y) + \dot{\omega}_{yc}\right.\\ & \left. + S_J(J_{\tilde{\omega}_y})c_2 x_1 - S_J(J_{u2})c_4 u_1\right]\end{aligned} \tag{35}$$

where $w_f(t)$ represents the loss of effectiveness for aileron δ_x with $w_f(t) = \begin{cases} 0, t \leq 1 \\ 1, t > 1 \end{cases}$.

In order to illustrate the performance of the proposed controller, numerical simulations are carried out to compare the performance of the proposed cooperative FTC scheme using interaction effect utilization (shortly called IEU-CFTC method) with standard decentralized control approach from (10)(shortly called standard DC method) and control allocation based FTC method (Alwi and Edwards (2008)) (namely CA-FTC) for system (34). In the simulation, the design parameters for IEU-CFTC are chosen as $\varepsilon = 0.02, \epsilon = 0.01, k_1 = 5, k_2 = 10, \eta_1 = 1, \eta_2 = 2$.

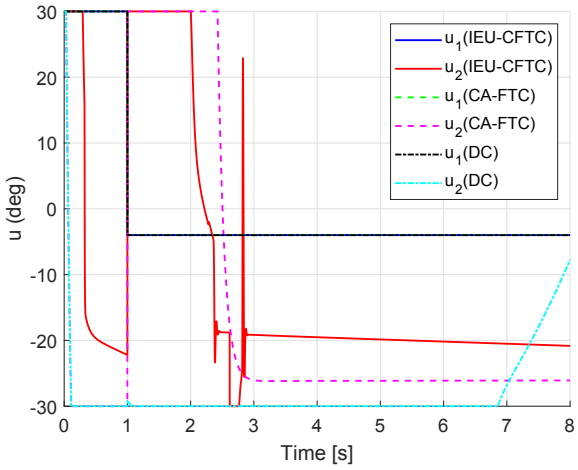

Fig. 3. Trajectories of the actuator deflection

The control gains for DC are $k_1 = 5, k_2 = 10$. The closed-loop eigenvalues for the nominal state feedback controller K based on CA associated with the healthy actuator δ_y are $\{-5, -10\}$.

The initial states of the missile are given by: $\omega_x(0) = -4\ rad/s, \omega_y(0) = 5\ rad/s$. The simulation results are shown in Fig. 1 to Fig.3, from which we can see that the system begins to diverge under the nominal decentralized control when one failure injected to aileron. It is observed from Fig. 1 that both the CA-FTC method and IEU-CFTC method render the closed-loop system converge to a small bound in finite time in the presence of one actuator failure. While, a better accuracy is obtained by using the IEU-CFTC approach than the CA-FTC from the local figure in Fig.1. The Fig. 2 illustrates that the virtual control works after the fault occurring at $t = 1\ s$ and becomes zero after the state x_1 converged in $t > 3\ s$. Moreover, the control inputs are plotted in Fig.3. It showed that a smoother actuator deflection in CA-FTC method than IEU-CFTC, while a less control effort used by IEU-CFTC approach.

5. CONCLUSIONS

In this context, an FTC scheme is presented for the nonlinear coupled system subjected to actuator faults, by utilizing the interaction effect. The proposed cooperative FTC approach can enforce and maintain the system tracking performance in the presence of actuator failure. It used the channel interconnection wisely and improved the fault-tolerant performance of a class of the MIMO nonlinear system. Simulation results obtained on the nonlinear lateral model of the attitude dynamics for one flight illustrate the benefits of the proposed scheme.

REFERENCES

Alwi, H. and Edwards, C. (2008). Fault tolerant control using sliding modes with on-line control allocation. *Automatica*, 44(7), 1859–1866.

Chang, J., Cieslak, J., Dvila, J., Zolghadri, A., and Zhou, J. (2017). Analysis and design of second-order sliding-mode algorithms for quadrotor roll and pitch estimation. *Isa Transactions*, 71(Pt 2), 495.

Chang, J., Guo, Z., and Cieslak, J. (2018). A fault tolerant control scheme for the reentry vehicle with reduced control effort. *IFAC-PapersOnLine*, 51(24), 812–817.

Chen, W., Ge, S.S., Wu, J., and Gong, M. (2015). Globally stable adaptive backstepping neural network control for uncertain strict-feedback systems with tracking accuracy knowna priori. *IEEE Transactions on Neural Networks and Learning Systems*, 26(9), 1842–1854.

Chwa, D.K. and Choi, J.Y. (2001). New parametric affine modeling and control for skid-to-turn missiles. *IEEE Transactions on Control Systems Technology*, 9(2), 335–347.

Dhadekar, D.D. and Patre, B.M. (2017). UDE-based decoupled full-order sliding mode control for a class of uncertain nonlinear MIMO systems. *Nonlinear Dynamics*, 88(1), 263–276.

Dickeson, J., Rodriguez, A., Sridharan, S., Benavides, J., and Soloway, D. (2009). Decentralized Control of an Airbreathing Scramjet-Powered Hypersonic Vehicle. In *AIAA Guidance, Navigation, and Control Conference*. American Institute of Aeronautics and Astronautics, Reston, Virigina.

Gao, G. and Wang, J. (2014). Observer-based fault-tolerant control for an air-breathing hypersonic vehicle model. *Nonlinear Dynamics*, 76(1), 409–430.

Guo, Z., Guo, J., Chang, J., and Zhou, J. (2018a). Coupling effect-triggered control strategy for hypersonic flight vehicles with finite-time convergence. *Nonlinear Dynamics*, 1–17.

Guo, Z., Guo, J., and Zhou, J. (2018b). Adaptive attitude tracking control for hypersonic reentry vehicles via sliding mode-based coupling effect-triggered approach. *Aerospace Science and Technology*, 78, 228–240.

Guo, Z., Zhou, J., Guo, J., Cieslak, J., and Chang, J. (2017). Coupling-Characterization-Based Robust Attitude Control Scheme for Hypersonic Vehicles. *IEEE Transactions on Industrial Electronics*, 64(8), 6350–6361.

Ra, C., Kim, S., Suk, J., Kim, Y., Moon, G., and Jun, B. (2013). Adaptive sliding mode autopilot design for skid-to-turn missile model with uncertainties. *IFAC Proceedings Volumes*, 46(19), 330–335.

Shen, Q., Jiang, B., and Shi, P. (2017). *Fault diagnosis and fault-tolerant control based on adaptive control approach*, volume 91. Springer.

Tian, B., Fan, W., Zong, Q., Wang, J., and Wang, F. (2013). Nonlinear robust control for reusable launch vehicles in reentry phase based on time-varying high order sliding mode. *Journal of the Franklin Institute*, 350(7), 1787–1807.

Weiland, C., Longo, J., Gülhan, A., and Decker, K. (2004). Aerothermodynamics for reusable launch systems. *Aerospace Science and Technology*, 8(2), 101–110.

Zolghadri, A., Henry, D., Cieslak, J., Efimov, D., and Goupil, P. (2014). *Fault Diagnosis and Fault-Tolerant Control and Guidance for Aerospace Vehicles*. Advances in Industrial Control. Springer London, London.